J|A|C|S
ARTICLES
Published on Web 09/30/2006

Reaction Intermediates in the Photoreduction of Oxygen Molecules at the (101) TiO_2 (Anatase) Surface

Giuseppe Mattioli, Francesco Filippone, and Aldo Amore Bonapasta*

Contribution from the Istituto di Struttura della Materia, Consiglio Nazionale delle Ricerche, Via Salaria km 29.5, CP 10, I-00016 Monterotondo Stazione, Roma, Italy

Received March 29, 2006; E-mail: aldo.amore@ism.cnr.it

Abstract: The structural, electronic, and vibrational properties of intermediates of the O_2 photoreduction at the (101) TiO_2 (anatase) surface have been investigated by performing ab initio density functional calculations. In detail, a recently proposed approach has been used where *molecules* on the surface are treated like *surface defects*. Thus, by applying theoretical methods generally used in the physics of semiconductors, we successfully estimate the location and donor/acceptor character of the electronic levels induced by an adsorbed molecule in the TiO_2 energy gap, both crucial for the surface−molecule charge-transfer processes, and investigate the formation and the properties of charged intermediates. The present approach permits a view of the O_2 photoreduction process through several facets, which elucidates the molecule−surface charge-transfer conditions and reveals the key role played by *charged intermediates*. A comparison of present results with those of a highly sensitive IR (infrared) spectroscopy study of intermediates of the O_2 photoreduction leads to a deeper understanding of this process and to revised vibrational-line assignments and reaction paths.

Introduction

In the last years, there has been a growing interest in applications of semiconductor metal oxides, in particular TiO_2, to photocatalytic processes such as the photooxidation of organic and small inorganic molecules in polluted air and water.[1−6] In these processes, O_2 molecules play a key role, being the species mainly involved in the photoreduction processes accompanying the photooxidation ones. Furthermore, O_2-derived oxidizing species are generally involved in the oxidation of organic compounds.[1−6] A rough description of the photocatalytic processes may include the following steps: (i) adsorption of a molecule on a semiconductor surface, (ii) photogeneration of electron−hole ($e-h$) pairs, (iii) trapping of electrons (holes) at surface sites, (iv) reduction (oxidation) of the adsorbed molecule through e (h) transfer from the surface to the molecule, (v) molecular desorption. Steps iii−v can be accompanied by the formation of reaction intermediates. Successful applications of photocatalysis require a full understanding of the microscopic processes underlying the above steps i−v, as shown by several experimental[1−6] and theoretical[7−14] studies. In this regard, a significant contribution has been given by a recent MIRIR (multiple internal reflection infrared spectroscopy) investigation of the O_2 photoreduction in acqueous solutions in contact with UV-irradiated TiO_2 rutile or anatase nanoparticles.[15] In that study, observed vibrational frequencies have been assigned to primary intermediates of the O_2 photoreduction, and mechanisms for this reaction have been proposed.

In the present paper, we investigate the above steps (i), (iv), and (v) of the O_2 photoreduction process by using ab initio density functional theory (DFT) methods. We focus on the formation and the structural, electronic, and vibrational properties of possible intermediates and compare our results with those of the MIRIR study. We use a recently proposed approach where molecules on a TiO_2 surface are treated like *surface defects* and investigated in the theoretical framework successfully used for *defects* in semiconductors.[16,17] For a given adsorbed molecule, such an approach permits *integration in a consistent picture* of the results concerning: (i) the strength of the surface−molecule interaction; (ii) the electronic properties of the surface−molecule system considered as a *whole*, thus including the location and the donor/acceptor character of the electronic levels induced by the adsorbed molecule in the energy gap of the semiconductor; (iii) the *charge-transfer* processes; (iv) the formation of neutral and *charged* intermediates; and (v) the vibrational properties of both neutral and charged species. A peculiar

(1) Hoffmann, M. R.; Martin, S. T.; Choi, W.; Bahnemann, D. W. *Chem. Rev.* **1995**, *95*, 69.
(2) Linsebigler, A. L.; Lu, G.; Yates, J. T., Jr. *Chem. Rev.* **1995**, *95*, 735.
(3) Mills, A.; Le Hunte, S. *J. Photochem. Photobiol., A* **1997**, *108*, 1.
(4) Fujishima, A.; Rao, T. N.; Tryk, D. A. *J. Photochem. Photobiol., C* **2000**, *1*, 1.
(5) Diebold, U. *Surf. Sci. Rep.* **2003**, *48*, 53.
(6) Carp, O.; Huisman, C. L.; Reller, A. *Prog. Solid State Chem.* **2004**, *32*, 33.
(7) Lindan, P. J. D.; Harrison, N. M.; Gillan, M. J. *Phys. Rev. Lett.* **1998**, *80*, 762.
(8) Vittadini, A.; Selloni, A.; Rotzinger, F. P.; Grätzel, M. *Phys. Rev. Lett.* **1998**, *81*, 2954.
(9) Sorescu, D. C.; Yates, J. T., Jr. *J. Phys. Chem. B* **2002**, *106*, 6184.
(10) Langel, W. *Surf. Sci.* **2002**, *496*, 141.
(11) Tilocca, A.; Selloni, A. *J. Chem. Phys.* **2003**, *119*, 7445.
(12) Zhang, C.; Lindan, P. J. D. *J. Chem. Phys.* **2003**, *118*, 4620.
(13) Zhang, C.; Lindan, P. J. D. *J. Chem. Phys.* **2003**, *119*, 9183.
(14) Tilocca, A.; Selloni, A. *Langmuir* **2004**, *20*, 8379.
(15) Nakamura, R.; Imanishi, A.; Murakoshi, K.; Nakato, Y. *J. Am. Chem. Soc.* **2003**, *125*, 7443.
(16) Van de Walle, C. G.; Neugebauer, J. *J. Appl. Phys.* **2004**, *95*, 3851.
(17) Amore Bonapasta, A.; Filippone, F. *Surf. Sci.* **2005**, *577*, 59.

10.1021/ja062145x CCC: $33.50

Table 1. Assignments of the Experimental Vibrational Frequencies to O_2 Photoreduction Intermediates As Proposed in the MIRIR Study (ref 15)[a]

	frequencies (cm^{-1})			pH		
species	ν_{O-O}	δ_{O-H}	ν_D	4.5	7.0	11.8
$Ti(O_2)$	943	–	931, 926[b]	s	s	s
Ti–OOH	838	–	770, 740[b]	w	no	no
Ti–OOH	–	1250–1120	900[c]	s	w	no
H_2O_2	887	–	–	s	no	no
H_2O_2	–	1250–1120	–	s	w	no
OOH·	1023	–	–	s	s	no

[a] ν_{O-O} and δ_{O-H} indicate stretching and bending frequencies, respectively. ν_D indicates frequencies estimated when substituting H with D. The experimental lines have a different strength when measured at different pH values: w = weak, s = strong, no = not observed. [b] The two frequencies are observed at pD equal to 11.2 and 6.5, respectively. [c] This frequency, not observed, could be masked by the ν_{O-O} band of $Ti(O_2)$.

advantage of such an approach is represented by the investigation of charged species, which are hardly discriminated from the neutral ones experimentally. Moreover, the present approach permits relating the formation of charged species to the position of the Fermi level in the semiconductors (i.e., to the doping conditions) as well as to the effects of the UV irradiation. In detail, neutral and charged intermediates have been investigated first in the form of free species in the vacuum. The properties of the free species have then been related to those of the same species adsorbed on the anatase surface, which give rise to a gas–solid system. In a third step, the effects of water molecules on the formation of intermediates and on the vibrational properties have been investigated in order to make the theoretical results appropriate for a comparison with MIRIR results. In this concern, we considered the stable (101) TiO_2 anatase surface,[18] that should be abundant in the anatase nanoparticles investigated in the MIRIR study. It may be also worth noticing that, in the same study, similar results were achieved for rutile and anatase nanoparticles, thus suggesting that the observed intermediates are related to general surface properties.

Present results clarify and enrich the picture given by the MIRIR results by indicating that *charged* intermediates play a key role in the O_2 photoreduction. In particular, they indicate a different assignment of some of the experimental lines and suggest different reaction mechanisms. They also suggest that the water molecules in contact with the TiO_2 surface give rise to quite short hydrogen bonds which significantly affect the H vibrational frequencies.

In the following, the results of the MIRIR study are summarized. Then, in the next sections, present theoretical results are discussed and compared with the experimental ones.

Observed vibrational lines are reported in Table 1 together with their assignments to reaction intermediates made in the MIRIR study. Such assignments have taken into account the variation of the measured frequencies induced by a change of the pH values or the substitution of H with D. Accordingly, it has been suggested that a surface peroxo, $Ti(O_2)$, and a hydroperoxo, Ti–OOH, are responsible for the two most important bands observed at 943 cm^{-1} and 1250–1120 cm^{-1}, respectively. Other lines are assigned to physisorbed H_2O_2 and OOH• radicals which, together with the $Ti(O_2)$ and Ti–OOH species, are involved in the reaction schemes proposed for the O_2 photoreduction; see Figure 1.

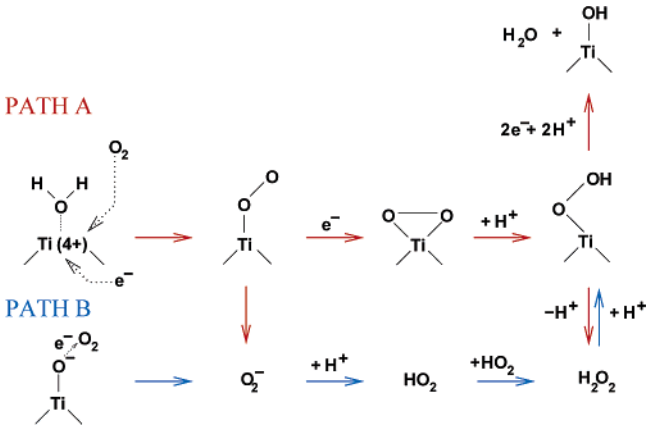

Figure 1. Reaction pathways for the O_2 photoreduction as proposed in the MIRIR study (ref 15).

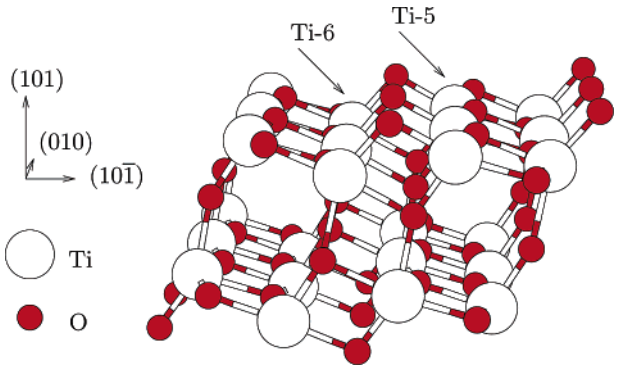

Figure 2. Structure of the (2 × 3) supercell used to simulate the anatase (101) surface. Five-fold- and six-fold-coordinated Ti surface atoms are labeled by Ti-5 and Ti-6, respectively.

Methods

Total energies, equilibrium geometries, and adsorption (desorption) enthalpies of different surface–molecule systems have been calculated by using DFT methods in the generalized gradient corrected approximation (GGA)[19–21] with the PBE exchange and correlation functional,[22] in the supercell approach. Ultrasoft pseudopotentials have been used for oxygen and titanium.[23,24] The supercells used to simulate molecules interacting with the (101) anatase surface have been obtained by adding ~7 Å of empty space to a bulk 72-atom supercell containing four (2 × 3) atomic layers (cell volume equal to 1688 $Å^3$); see Figure 2. Geometry optimization procedures have been performed by fully relaxing the positions of all of the atoms of a supercell, except for the atoms of the fourth layer (formed by the lowest twelve O atoms and six Ti atoms) which have been kept fixed to their optimized bulk positions.

Total energy values have been used to estimate the strength of a molecule–surface interaction through the calculation of desorption enthalpies, e.g., in the case of an O_2 molecule:

$$\Delta H_{des}(O_2) = E(O_2 - Surf) - E(Surf) - E(O_2)$$

where the total energy values are relative to supercells simulating an O_2 molecule interacting with the anatase surface, the surface, and an isolated O_2 molecule in the vacuum, respectively. Present estimates of

(18) Lazzeri, M.; Vittadini, A.; Selloni, A. *Phys. Rev. B* **2001**, *63*, 155409.
(19) Hohenberg, P.; Kohn, W. *Phys. Rev.* **1964**, *136*, B864.
(20) Kohn, W.; Sham, L. J. *Phys. Rev.* **1965**, *140*, A1133.
(21) Car, R.; Parrinello, M. *Phys. Rev. Lett.* **1985**, *55*, 2471.
(22) Perdew, J. P.; Burke, K.; Ernzerhof, M. *Phys. Rev. B* **1996**, *77*, 3865.
(23) Vanderbilt, D. *Phys. Rev. B* **1990**, *41*, 7892.
(24) Laasonen, K.; Pasquarello, A.; Lee, C.; Car, R.; Vanderbilt, D. *Phys. Rev. B* **1993**, *47*, 10142.

$\Delta H_{(des)}(H_2O)$ and $\Delta H_{(des)}(O_2)$, −0.72 and −0.34 eV, respectively, are close to those estimated in previous theoretical and experimental studies.[8,17,25]

A careful analysis of the electronic properties of a molecule−surface system has been performed by investigating electronic eigenvalues at the Γ point, *defect formation energies* and *transition energy levels*.[16,26,27] The two last quantities involve both *neutral* and *charged* systems and permit estimating the *location* in the anatase energy gap and the *character* (donor or acceptor) of the electronic levels induced by an adsorbed molecule, both playing a key role in the *charge-transfer* processes. In agreement with the present theoretical approach, the charge of an adsorbed molecule is defined like that of a defect in a semiconductor. Thus, when a surface−molecule charge-transfer occurs, the degree of localization of electronic charge on the adsorbed molecule is directly related to the location and the character of the electronic level induced by the molecule itself. This implies a strong (weak) localization in the case of deep (shallow) electronic levels (see also the Supporting Information).

In a supercell approach, the formation energy $\Omega(M_{ads}{}^q)$ of an adsorbed M_{ads} molecule carrying a q charge is estimated like that of a defect by:

$$\Omega(M_{ads}{}^q) = E(M_{ads}{}^q) - E(Surf) - \mu_M + q(\mu_F + E_{VB})$$

where $E(M_{ads}{}^q)$ and $E(Surf)$ are the total energies of a supercell simulating a TiO_2 surface with and without a charged absorbed molecule $M_{ads}{}^q$, respectively, μ_M is the free-molecule chemical potential, assumed equal to the energy of an M molecule in the vacuum, and q is the negative (positive) charge on the M_{ads}, i.e., the number of electrons transferred to (from) the molecule from (to) an electron reservoir with a chemical potential, namely, a Fermi level, μ_F. $\mu_F = 0$ corresponds to the valence band maximum (VBM) of bulk anatase. This choice also requires explicit inclusion of the energy of VBM, E_{VB}, in the estimate of $\Omega(M_{ads}{}^q)$. In the case of charged states, the estimate of the defect formation energies requires some correction terms (as described in ref 16), estimated here but not shown in the above expression. A transition energy level $\epsilon^{n/n+1}(M_{ads})$ is defined as the Fermi-level position where the charge states n and $n + 1$ of an M_{ads} molecule have equal formation energy, that is, the Fermi level where both charge states exist and an electronic transition at the level induced by the molecule in the energy gap can occur. Transition energy levels can be observed in experiments where the final charge state relaxes to its equilibrium configuration after the transition. Moreover, transition energy levels permit one to estimate the predominant charge state of an adsorbed molecule at a given value of the Fermi energy, that is, its donor or acceptor character. These levels must be compared to the energy band gap E_g, estimated here as the difference between the electron affinity and the ionization potential calculated for the perfect surface. Such an approach permits comparison of consistent results. The present estimate of E_g is 2.89 eV, to be compared with an experimental value of 3.28 eV.[28] Finally, a finite-difference calculation method has been used to estimate the vibrational frequencies (in the harmonic approximation) related to the topmost layers of the molecule−surface system. Geometry optimizations and vibrational analyses have been performed by using the CPMD code,[29] electronic properties have been investigated by using the Quantum-ESPRESSO package.[30]

Table 2. O−O Equilibrium Distances and Stretching Vibrational Frequencies (ν_{O-O}) Calculated for Free (Square Bracketed) and Adsorbed (Not Bracketed) Neutral and Charged O_2 Molecules[a]

species	O–O (Å)	ν_{O-O} (cm^{-1})
$[O_2]$	1.24	1565
$[O_2^-]$	1.33	1132
$[O_2^{-2}]$	1.34	1098
O_2	1.25	1467
O_2^-	1.33	1194
O_2^{-2}	1.46	958

[a] Geometries of the adsorbed molecules are shown in Figure 3. Charged molecules form surface peroxo species.

Results

In the next sections, results are presented for different charged and neutral intermediates of the O_2 photoreduction. Special care was given to the results achieved for the H_2O_2 molecule in order to illustrate the combined effects of surface and water molecules on the H vibrational modes of that molecule.

O_2 Peroxo Groups. First, the geometry and vibrational frequency of the $[O_2]$, $[O_2^-]$, and $[O_2^{-2}]$ free molecules in the vacuum have been investigated; see Table 2 (hereafter, free molecular species will be identified by square brackets in order to distinguish them from species adsorbed on the surface). The O−O bond distance and the stretching frequency of $[O_2]$ are in a good agreement with the experimental values of 1.21 Å and 1580 cm^{-1}, respectively.[31] The $[O_2]$, $[O_2^-]$, and $[O_2^{-2}]$ molecules show increasing O−O bond distances and decreasing O−O-stretching frequencies, also in agreement with the experimental findings.[31] Then, the bonding of an adsorbed O_2 molecule has been investigated by optimizing the geometry of a molecule located at different sites of the anatase surface. The minimum energy configuration has been found for an O_2 molecule located upon a five-fold coordinated Ti^{4+} surface ion; see Figure 3A. The O_2 molecule weakly binds to the Ti ion as shown by a desorption enthalpy $\Delta H_{des}(O_2)$ of −0.34 eV (hereafter, negative Δ-quantities, enthalpies or energies, indicate endothermic processes) and Ti−O bond distances of 2.31 and 3.19 Å to be compared with Ti−O distances of about 2.0 Å in the anatase bulk. Although weakly bound, the O_2 molecule induces an occupied and an empty states in the anatase energy gap corresponding to electronic eigenvalues located at 0.60 and 0.89 eV above VBM, respectively. The latter electronic state suggests an acceptor behavior of the adsorbed molecule. We have considered, therefore, the filling of this empty level and investigated the properties of the O_2^- and O_2^{-2} ion molecules adsorbed at the same Ti site.

Parts B and C of Figure 3 show the equilibrium geometries of these two ion molecules. The corresponding formation energies, $\Omega(O_2^-)$ and $\Omega(O_2^{-2})$, are shown as functions of the Fermi energy in Figure 4 together with the formation energy of the neutral molecule, $\Omega(O_2^0)$. In this figure, the intersections between $\Omega(O_2^0)$ and $\Omega(O_2^-)$ and between $\Omega(O_2^-)$ and $\Omega(O_2^{-2})$ give the transition levels $\epsilon^{0/-1}$ and $\epsilon^{-1/-2}$, which are located at 0.92 and 1.44 eV from VBM, respectively. This result confirms that an adsorbed O_2 molecule induces an acceptor electronic level in the energy gap, which can be doubly occupied when the Fermi level is close to $E_g/2$ (i.e., 1.45 eV in undoped anatase). The electrons occupying this acceptor level are mainly

(25) Herman, G. S.; Dohnàlek, Z.; Ruzycki, N.; Diebold, U. *J. Phys. Chem. B* **2003**, *107*, 2788.
(26) Amore Bonapasta, A.; Filippone, F.; Giannozzi, P.; Capizzi, M.; Polimeni, A. *Phys. Rev. Lett.* **2002**, *89*, 216401.
(27) Van de Walle, C. G.; Neugebauer, J. *Nature* **2003**, *423*, 626.
(28) Forro, L.; Chauvet, D.; Emin, L.; Zuppiroli, L.; Berger, H.; Levy, F. *J. Appl. Phys.* **1994**, *75*, 633.
(29) *CPMD* V3.9; IBM Corp 1990−2005; MPI fuer Festkoerperforshung Stuttgart 1997−2001; http://www.cpmd.org
(30) Baroni, S.; Dal Corso, A.; de Gironcoli, S.; Giannozzi, P.; Cavazzoni, C.; Ballabio, G.; Scandolo, S.; Chiarotti, G.; Focher, P.; Pasquarello, A.; Laasonen, K.; Trave, A.; Car, R.; Marzari, N.; Kokalj, A. http://www.pwscf.org/.
(31) Cotton, F. A.; Wilkinson, G. *Advanced Inorganic Chemistry*; Wiley-Interscience: New York, 1988.

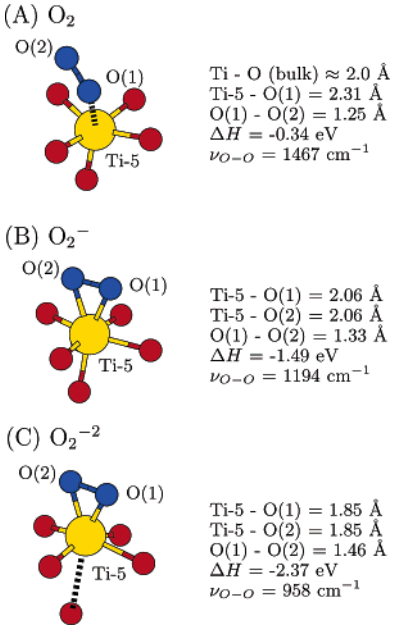

Figure 3. Optimized geometries, desorption enthalpies, and O−O-stretching frequencies (ν_{O-O}) of: (A) O_2, (B) O_2^-, and (C) O_2^{-2} molecules adsorbed on a surface five-fold-coordinated Ti site. O_2^- and O_2^{-2} correspond to surface peroxo species.

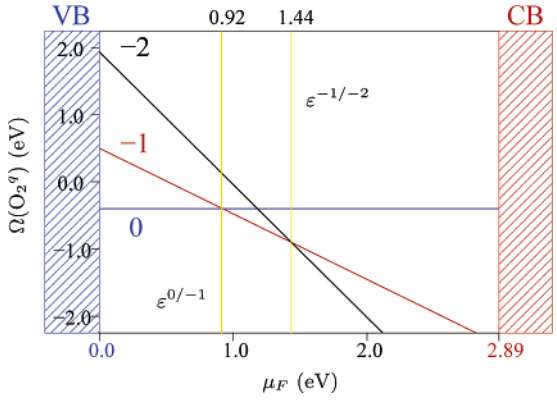

Figure 4. Formation energies of adsorbed O_2 molecules carrying a charge q equal to 0, −1, −2 (see the line labels), as functions of the Fermi energy, μ_F. Intersections between formation energies give the *transition energy level* ($\epsilon^{n/n+1}$) between the n and $n+1$ charged states.

localized on the O_2 molecule as shown by the dramatic changes of geometry and chemical bonding observed when going from the neutral to the charged molecules. In the O_2^- and O_2^{-2} ion molecules, the two oxygen atoms are indeed *both* bonded to a Ti atom in a symmetric configuration (see B and C of Figure 3 and compare with Figure 3A) thus forming *charged peroxo groups* (see also the Supporting Information). In these charged groups, the Ti−O distances are close to those in the bulk anatase and appreciably shorter than those estimated for the adsorbed neutral molecule. This indicates the formation of strong Ti−O bonds as confirmed by desorption enthalpies $\Delta H_{(des)}(O_2^-)$ and $\Delta H_{(des)}(O_2^{-2})$ equal to −1.49 eV and −2.37 eV, respectively.[32] Thus, present results support an acceptor character of the adsorbed O_2 molecules and their capability of acting as electron traps, in agreement with suggestions given by the experiments.[4,6,15,33,34] On the other hand, the above results suggest that adsorbed O_2^- and O_2^{-2} ion molecules are hardly detached from the surface in a gas−solid system.

A full vibrational analysis has been performed for the molecule−surface systems shown in Figure 3. The O−O-stretching frequencies for the O_2, O_2^-, and O_2^{-2} adsorbed molecules are equal to 1467, 1194, and 958 cm^{-1}, respectively; see Table 2. In the O_2, O_2^-, and O_2^{-2} adsorbed molecules, increasing O−O distances are accompanied by decreasing O−O-stretching frequencies, thus paralleling the case of the free molecules; see Table 2. These results are consistent with an electron transfer from the surface to the O_2 molecule.

H_2O_2 Molecules. Even in the case of H_2O_2, the structure and vibrational properties of a free molecule have been investigated first; see [H_2O_2] in Table 3. The calculated O−O and O−H distances, 1.48 and 0.97 Å, are respectively close to the experimental values of 1.47 and 0.97 Å.[31] Present estimates of the O−O-stretching and H-bending and -stretching frequencies are also in a very good agreement with the experiment (molecules in gas phase in Table 3).[35] The comparison of calculated vibrational frequencies with the experimental ones has been extended to the case of molecules in a water solution, simulated here by considering a H_2O_2 molecule surrounded by four H_2O molecules ([H_2O_2] + $n H_2O$ in Table 3). The achieved results are once more in a quite good agreement with the experiment (molecules in liquid phase).[35] In particular, the theoretical results show the formation of H bonds between the H atoms of the [H_2O_2] molecule and the O atoms of the water molecules having a typical length of about 1.8−1.9 Å.[37] These H bonds are responsible for the observed weakening (strengthening) of the H-stretching (bending) modes in the case of [H_2O_2] + $n H_2O$ with respect to the free [H_2O_2] molecule. Interestingly, these H bonds induce also the appearance of two new H-bending modes, δ'_{O-H} in Table 3, at 625 and 821 cm^{-1}. These modes are not observed experimentally. However, modes around 800 cm^{-1} are observed in the case of solid H_2O_2; see Table 3.[35] This suggests that the δ'_{O-H} modes may be precursors of the modes observed in the solid phase, likely related to hindered rotations of the H_2O_2 molecule surrounded by interacting molecules. The isotopic shifts of the above H_2O_2 vibrational frequencies due to the H substitution with D also agree with the experimental findings (molecules in Ar matrix);[36] see Table 3.

The minimum energy configuration of a H_2O_2 molecule interacting with the anatase surface (as in a gas−solid system) is shown in Figure 5 A. The adsorbed H_2O_2 molecule induces a fully occupied state in the anatase energy gap, compatible with photooxidation processes which are beyond the scope of the present work. Thus, we consider here only the case of the neutral, adsorbed molecule. The corresponding $\Delta H_{(des)}(H_2O_2)$, −0.64 eV, is larger than $\Delta H_{(des)}(O_2)$ because a H bond forms between the H_2O_2 molecule and a surface O atom; see Figure 5. This H bond has effects on the vibrational frequencies of the H_2O_2 molecule similar to those induced by the H bonds in the [H_2O_2] + $n H_2O$ case discussed above. This result has raised our attention on the combined effects that both the TiO_2 *surface*

(32) Quite larger values were reported in ref 17 due to an intrinsic overestimation of the $\Delta H_{(des)}$ values.
(33) Nakamura, R.; Nakato, Y. *J. Am. Chem. Soc.* **2004**, *126*, 1290.
(34) Zubkhov, T.; Stahl, D.; Thompson, T. L.; Panayotov, D.; Diwald, O.; Yates, J. T., Jr. *J. Phys. Chem. B* **2005**, *109*, 15454.
(35) Miller, R. L.; Hornig, D. F. *J. Chem. Phys.* **1961**, *34*, 265.
(36) Engdahl, A.; Nelander, B.; Karlström, G. *J. Phys. Chem. A* **2001**, *105*, 8393.
(37) Head-Gordon, T.; Hura, G. *Chem. Rev.* **2002**, *102*, 2651.

Table 3. Vibrational Frequencies Calculated for Free H_2O_2, HDO_2, and D_2O_2 Molecules (Square Bracketed) Are Given in the Upper Part of the Table; They Can Be Compared with the Experimental Data Given in the Lower Part; the Middle Part of the Table Reports Results Achieved for Adsorbed H_2O_2 and D_2O_2 Molecules (Not Bracketed); $n$$H_2O$ ($n$$D_2O$) Indicates That Few (three or four) H_2O (D_2O) Molecules Surround the Investigated Species; H_2O-*layer* Indicates That a H_2O_2 Molecule Is Inserted in a Layer of 23 Water Molecules; *X*/*Y* Represents Two Distinct *X* and *Y* Vibrational Modes of the H_2O_2 Molecule, Whereas *X*−*Y* Represents a Doublet Peak; the Vibrational Modes of Water Molecules Are not Reported; ν_{O-O}, δ_{O-H}, and ν_{O-H} Indicate O−O-Stretching, O−H (or O−D)-Bending, and O−H (or O−D)-Stretching Frequencies, Respectively; δ'_{O-H} Modes Are Peculiar Bending Modes Induced by Water Molecule or Combined Surface and Water Molecule Effects

	frequencies (cm^{-1})			
species	ν_{O-O}	δ_{O-H}	ν_{O-H}	δ'_{O-H}
$[H_2O_2]$	893	1268/1366	3650/3651	–
$[H_2O_2]H_2O$	894	1397/1434	3241/3405	625/821
$[HDO_2]$	892	961/1313	2669/3652	–
$[D_2O_2]$	890	937/1001	2665/2669	–
$[D_2O_2] + nD_2O$	892	1016/1065	2372/2487	459/597
H_2O_2	893	1266/1458	3631/3320	–
$H_2O_2 + nH_2O$	898	1515/1630	2481/3327	1184
$D_2O_2 + nD_2O$	898	1072/1155	1792/2426	822
$H_2O_2 + H_2O$-*layer*	897	1528/1583	2777/2992	1197
		Experimental Data		
H_2O_2 IR *gas*[a]	877	1266/1315	3610/3614	–
H_2O_2 IR, Raman *liquid*[a]	880	1350/1400	3400/3400	–
H_2O_2 IR *crystal*[a]	882	1385/1407	3192/3285	650/808
$[H_2O_2]$ IR *Ar matrix*[b]	867 (*c*)	1271−1277	3588−3597	–
$[HDO_2]$ IR *Ar matrix*[b]	–	981/1343−1350	2646−2651/3587−3588	–
$[D_2O_2]$ IR *Ar matrix*[b]	–	952	2645−2646	–

[a]Reference 35. [b]Reference 36. [c]H_2O_2 dimer.

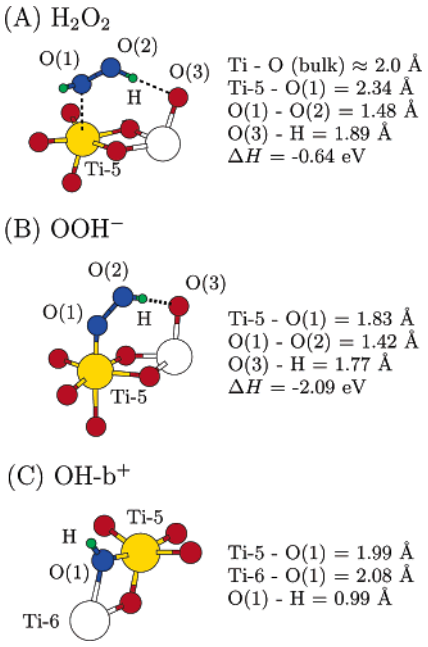

Figure 5. Optimized geometries and desorption enthalpies of: (A) an adsorbed H_2O_2 molecule; (B) an adsorbed OOH^- group; and (C) an OH-b^+ bridging hydroxyl group.

and *water* molecules may have on the H vibrational frequencies of an adsorbed H_2O_2 molecule. Therefore, a preliminary investigation concerned the structure and the vibrational frequencies of an adsorbed H_2O_2 molecule surrounded by four water molecules in contact with the surface; see $H_2O_2 + nH_2O$ in Table 3. Interestingly, the structure of such a system shows that a *peculiar* H bond forms between a H atom of H_2O_2 and a surrounding water molecule. This H bond is characterized by a H−O distance of 1.52 Å, sizably *shorter* than the usual distance of about 1.9 Å.[37] The other H atom of H_2O_2 is involved in a H bond of 1.86 Å with another water molecule. These two H bonds have significant effects on the H-bending frequencies of the isolated, adsorbed H_2O_2, the 1266 and 1458 cm^{-1} frequencies of this molecule being raised to the values of 1515 and 1630 cm^{-1}. Moreover, a new H-bending frequency appears at 1184 cm^{-1}, which recalls the δ'_{O-H}-bending modes induced by the H bonds in the above case of $[H_2O_2] + nH_2O$. The above H bonds do not affect instead the O−O-stretching frequency of H_2O_2.

Results concerning the origin of the above short H bonds will be reported elsewhere (preliminary results are given in the Supporting Information).[38] These results support the existence of short H bonds when water molecules are in contact with the TiO_2 surface. Then, we have reinvestigated the vibrational frequencies of a H_2O_2 molecule adsorbed on the anatase surface and included in an overlayer (two bilayers) of 23 H_2O molecules ($H_2O_2 + H_2O$-*layer* in Table 3). The achieved results closely agree with those obtained in the $H_2O_2 + nH_2O$ system. This further supports the above results and indicates that the effects of H bonds on the vibrational frequencies of an adsorbed molecule can be simulated by surrounding the molecule with a small number of H_2O molecules close to the surface.

Hydroperoxo Groups. In the case of hydroperoxo intermediates, the properties of free [OOH•] and [OOH^-] species have been investigated first; see Table 4. Then, the case of hydroperoxo species surrounded by water molecules has been considered in order to investigate the effects of H bonds on the vibrational properties. The case of an [OOH•] radical surrounded by water molecules ([OOH•] + nH_2O in Table 4) has been investigated with a particular care because artificial bonding configurations have been found by DFT-PBE investigations in the case of the [OH•] + nH_2O system.[39,40] Present results show that such artificial configurations do not form in the case of OOH• radicals. They also show that, in the case of [OOH•] + nH_2O, the hydroperoxo H atom forms a short hydrogen bond

(38) Unpublished results.
(39) Vassilev, P.; Louwerse, M. J.; Baerends, E. J. *Chem. Phys. Lett.* **2004**, *398*, 212.
(40) VandeVondele, J.; Sprik, M. *Phys. Chem. Chem. Phys.* **2005**, *7*, 1363.

Table 4. O−O Equilibrium Distances and O−O and H Vibrational Frequencies Calculated for Free (Square Bracketed) and Adsorbed (Not Bracketed) Neutral and Charged OOH and OOD Species[a]

species	O–O (Å)	frequencies (cm^{-1})			
		ν_{O-O}	δ_{O-H}	ν_{O-H}	δ'_{O-H}
[OOH•]	1.34	1119	1344	3420	−
[OOH^-]	1.49	755	1118	3604	−
[OOH•] + $n H_2O$	1.35	1152	1600	2633	1003
[OOD•]	1.34	1147	981	2501	−
[OOD^-]	1.49	734	856	2637	−
[OOD•] + $n D_2O$	1.35	1147	1168	1926	739
OOH	1.36	1160	1392	2251	1032
OOH^-	1.42	1017	1453	3156	−
OOH^- + $n H_2O$	1.44	971	1558	2517	1151
OOD^- + $n D_2O$	1.44	964	1126	1841	802

[a] nH_2O (nD_2O) indicates that few (three or four) H_2O (D_2O) molecules surround the investigated species. The vibrational modes of water molecules are not reported. ν_{O-O}, δ_{O-H}, and ν_{O-H} indicate O−O-stretching, O−H (or O−D)-bending, and O−H (or O−D)-stretching frequencies, respectively. δ'_{O-H} modes are peculiar bending modes induced by water molecule or combined surface and water molecule effects.

(1.54 Å) with one of the surrounding molecules which has effects similar to those discussed in the case of adsorbed H_2O_2. In particular, a new δ'_{O-H}-bending frequency appears at 1003 cm^{-1}. At variance with the case of neutral hydroperoxo, the presence of charged [OOH^-] species in a water solution is unlikely, unless the pH is very high. This ionic species spontaneously reacts indeed with a H_2O molecule by forming a H_2O_2 molecule and an [OH^-] ion. Isotopic shifts of the vibrational frequencies of the above OOH species are also given in Table 4.

Surface-bound hydroperoxo groups have then been investigated; see Table 4. The minimum energy configuration of the neutral OOH is similar to that shown in Figure 5B for the charged OOH^- and is characterized by a short hydrogen bond (1.51 Å) with a surface O atom induced by surface effects such as the short H bonds reported above for adsorbed H_2O_2 molecules.

The electronic structure of the surface OOH group is characterized by a half-occupied electronic eigenvalue located in the energy gap at 0.16 eV from VBM, which suggests an acceptor behavior of this group. The structure of a negatively charged OOH^- group has been therefore investigated, and the corresponding equilibrium geometry is shown in Figure 5B. The OOH^- ion is tightly bonded to the surface as shown by a short Ti−O distance of 1.83 Å and by a $\Delta H_{(des)}(OOH^-)$ of −2.09 eV. This group is also characterized by an O−O bond distance close to that found for the free [OOH^-] ion (see Table 4) and by a hydrogen bond with an O surface atom having a H−O distance of 1.77 Å. The formation energies of the OOH and OOH^- absorbed species, $\Omega(OOH^0)$ and $\Omega(OOH^-)$, respectively, as functions of the Fermi energy give a transition level $\epsilon^{0/-1}$ located at 0.87 eV above VBM. This result confirms the acceptor character of the adsorbed OOH group and indicates that it will be negatively charged in semi-intrinsic anatase, thus behaving like an adsorbed O_2 molecule.

The vibrational properties of the above hydroperoxo groups are given in Table 4. In the cases of free and adsorbed molecules, the achieved results are similar to those discussed above for the H_2O_2 molecules. The presence of surrounding water molecules has instead peculiar effects on the properties of the adsorbed OOH and OOH^- species. In the presence of water molecules, the OOH is unstable, and it loses its H atom by forming a H_3O^+ ion and a surface O_2^- peroxo species. This is a significant result because it indicates that OOH• radicals *should not be released* by the anatase surface in contact with aqueous solutions. In the case of surface OOH^-, the water molecules induce only a significant rearrangement of its structure. In the new configuration, a hydrogen bond forms between the H of the hydroperoxo group and the O atom of a surrounding H_2O molecule in place of a surface O atom. Moreover, the new hydrogen bond is characterized by a short O−H distance of 1.57 Å. This peculiar hydrogen bond has the same origin as that of the short H bonds reported above for the H_2O_2 molecule and has also similar effects on the H-bending modes; see OOH^- and OOH^- + nH_2O in Table 4. In particular, the H-bending frequency of 1453 cm^{-1} is increased to 1558 cm^{-1}, and a new δ'_{O-H} mode appears at 1151 cm^{-1}. The O−O-stretching frequency is slightly lowered from 1017 to 971 cm^{-1}.

Table 5. Vibrational Frequencies Calculated for OH-b (OD-b) Bridging and OH-t (OD-t) Terminal Hydroxyl Groups in Different Charged States; nH_2O (nD_2O) Indicates That Few (three or four) H_2O (D_2O) Molecules Surround the Investigated Species; the Vibrational Modes of Water Molecules Are not Reported; δ_{O-H} and ν_{O-H} Indicate O−H (or O−D)-Bending and O−H (or O−D)-Stretching Frequencies, Respectively; δ'_{O-H} Modes Are Peculiar Bending Modes Induced by Water Molecule and Combined Surface and Water Molecule Effects

species	frequencies (cm^{-1})		
	δ_{O-H}	ν_{O-H}	δ'_{O-H}
OH-b	751	3815	−
OH-b^+	820	3802	−
OD-b^+	547	2761	−
OH-b^+ + nH_2O	1075	2979	1014
OD-b^+ + nD_2O	752	2165	696
OH-t	1100	4135	−
OH-t^-	756	3778	−
OH-t^- + nH_2O	1050	3379	822
OD-t^- + nD_2O	769	2467	595

Surface OH Groups. A bridge OH group (OH-b) is a two-fold coordinated OH group involving a surface O-bridge atom and characterized by a structure similar to that shown in Figure 5C for the charged OH-b^+ group. The electronic structure of the neutral OH-b group is characterized by a half-occupied electronic eigenvalue located at 0.13 eV below the minimum of the conduction band (CBm), which suggests a donor behavior of this group. The properties of the positively charged OH-b^+ have been therefore investigated. In particular, an $\epsilon^{+1/0}$ transition level located at 2.43 eV from VBM has been estimated from the Ω(OH-b^0) and Ω(OH-b^{+1}) formation energies. This result confirms the donor character of the OH-b group, which will be positively charged in the case of undoped anatase.

The vibrational frequencies estimated for OH-b and OH-b^+ are reported in Table 5. In the case of OH-b^+ surrounded by water molecules, a quite strong hydrogen bond with a H−O distance of 1.59 Å forms between the H atom of the group and the O atom of a H_2O molecule. This hydrogen bond has significant effects on the H frequencies as in the case of the short H bonds reported above. In particular, it strengthens (weakens) the original H-bending (stretching) frequency and induces the appearance of a new δ'_{O-H}-bending mode with a frequency of 1014 cm^{-1}; see Table 5.

The properties of terminal OH surface groups having the O atom bonded to a Ti surface atom, OH-t, have been also

investigated. These OH-t groups behave as strong acceptors, forming OH-t$^-$ groups in undoped anatase. However, the vibrational frequencies calculated for the charged OH-t$^-$ groups have no an experimental counterpart at high values of pH where these groups should be strongly favored; see, for example, the bending modes at 822 and 1050 cm^{-1} in Table 5. This indicates that OH-t surface groups do not play a significant role in the O_2 photoreduction.

Discussion

The MIRIR vibrational lines can be roughly divided in lines sensitive to different values of pH or to the H−D substitution, that is, related to H-containing groups, or not. Accordingly, present theoretical results will be discussed by separating surface groups involving H atoms from those involving only O_2 molecules and Ti surface atoms (e.g., peroxo groups). A final section will report concluding remarks and summarize the differences between the assignment of the vibrational lines and the reaction schemes proposed here and in the MIRIR study.

Peroxo Groups. In the MIRIR study, the initial step of the O_2 photoreduction involves the formation of a surface superoxo, Ti−OO, followed by that of a surface peroxo group, Ti(O_2); see path A in Figure 1. Although electronic transfers are assumed in that reaction path, no indication is given about the charge of the superoxo and peroxo groups. Present results agree only in part with that scheme of reaction. First, they show that a surface superoxo does not develop into either a neutral or into a negatively charged form. In the former case, an oxygen molecule interacts too weakly with the surface. In the latter, the charged O_2 molecule forms a charged peroxo group. On the other hand, present results show that the weakly bound O_2 molecule behaves as a strong acceptor by inducing an unoccupied electronic level in the anatase energy gap. This leads to an easy reduction of the adsorbed molecule that forms a surface O_2^{-2} peroxo group carrying a *double* negative charge; see Figure 3. The O_2^{-2} can form in undoped TiO_2 because the corresponding $\epsilon^{-1/-2}$ transition level is close to $E_g/2$. This implies that O_2^{-2} surface groups *may exist in the dark and become the predominant species when UV irradiation increases the density of photogenerated electrons*. Regarding the vibrational properties of the surface peroxo species preliminarily, it has to be noted that a very good agreement is found between present estimates of the O−O-stretching frequencies and the corresponding experimental values in the cases of free (gaseous) O_2 and H_2O_2 molecules. This makes us confident about the vibrational frequencies estimated here for O_2-related surface groups. In the case of the peroxo-like groups, these estimates show that only the charged O_2^{-2} surface peroxo presents an O−O-stretching frequency of 958 cm^{-1} in a very good agreement with the observed frequency of 943 cm^{-1}. This result substantially agrees with the assignment to peroxo species made in the MIRIR study. However, it has to be stressed that the charge of the O_2^{-2} peroxo has significant consequences. First, in aqueous solutions, a negative doubly charged peroxo group strongly attracts H^+ ions, thus favoring the formation of hydroperoxo groups which can also play an important role in the photocatalytic process, as will be discussed in the next sections. Second, in a gas−solid system, O_2^{-2} ions are hardly detached from the surface. Possibly, the capture of a hole at the peroxo site may favor the release of a O_2^- group, although a $\Delta H_{(des)}(O_2^-)$ of −1.49 eV seems too high for the O_2^- detachment. This may affect the role of the highly reactive O_2^- species in photocatalytic processes in gaseous phases.

The formation of O_2^{-2} peroxo species was also predicted in a previous study on a different (100) anatase surface.[17] This suggests that the formation of O_2^{-2} species and their related effects are general features of the O_2−anatase surface interaction.

Hydroperoxo Groups and H_2O_2 Molecules. The experimental vibrational lines reported in Table 1 can be also divided in four main groups: (i) the 838 and 887 cm^{-1} lines, (ii) the 943 cm^{-1} line, (iii) the 1250−1120 cm^{-1} band, and (iv) a 1023 cm^{-1} line. The 943 cm^{-1} line was assigned to surface peroxo species as discussed above. The formation of OOH groups and H_2O_2 molecules (resulting from further protonation of the OOH groups) was proposed instead, in the MIRIR study, to account for the other vibrational lines. In particular, the bands observed at 838 and 887 cm^{-1} were assigned to the O−O-stretching modes of surface OOH and physisorbed H_2O_2, respectively. The 1250−1120 cm^{-1} band was assigned to H-bending modes related to the surface OOH group and/or the H_2O_2 molecule. The 1023 cm^{-1} line was assigned to the O−O-stretching mode of hydroperoxo radicals present in the solution phase; see path B in Figure 1. The species involving H atoms were carefully investigated in the MIRIR study by considering the effects of both different pH values and H substitution with D on the vibrational spectra. Regarding the pH effects, all of the above lines are observed at pH 4.5; a similar spectrum is observed at pH 7.0, except for the disappearance of the lines at 838 and 887 cm^{-1} and a weakening of the 1250−1120 cm^{-1} band, whereas only the line at 943 cm^{-1} is observed at pH 11.8 (see Table 1). These pH effects seem to support the above assignments and the formation of hydroperoxo species and H_2O_2 molecules favored by the presence of H^+ ions, as indicated in the paths A and B of Figure 1. In the case of H−D exchange, MIRIR spectra at pD 6.5 and 11.2 show a predominant band at 926−931 cm^{-1} and a second band at 740−770 cm^{-1}. Then, it was proposed that the line at 943 cm^{-1} assigned to the O−O-stretching frequency of the surface peroxo group has slight isotopic shifts, thus corresponding to the band at 926−931 cm^{-1} in D_2O. The bands assigned to surface OOH groups at 838 cm^{-1} (O−O-stretching band) and 1250−1120 cm^{-1} (H-bending band) should shift to the bands at 740−770 cm^{-1} and around 900 cm^{-1}, respectively, for OOD. Regarding the 1023 cm^{-1} line, it is only reported that it is sensitive to the H−D exchange. Finally, no comment is given on possible isotopic shifts of the 887 cm^{-1} line.

On the side of theory, we start our discussion with the results achieved for the H_2O_2 molecules. The above assignment of the 887 cm^{-1} frequency to the O−O-stretching mode of the H_2O_2 molecule is in a very good agreement with the present estimate of 898 cm^{-1} for $H_2O_2 + nH_2O$; see Table 3. The 1184 cm^{-1} value calculated for a H-bending mode in H_2O_2 also agrees with the assignment proposed for the observed 1250−1120 cm^{-1} band. The two further H-bending frequencies estimated at 1515 and 1630 cm^{-1} for the H_2O_2 molecules have no an experimental counterpart. They are located at the boundaries or outside of the range of the measured spectra and possibly masked by the H_2O-bending frequencies.[15] Moreover, these frequencies could

contribute to the experimental band observed at 1613 cm-1 (Figure 4 of the MIRIR study). Regarding the H−D exchange, none of the isotopic shifts estimated for the $H_2O_2 + nH_2O$ vibrational frequencies has an experimental counterpart (see Table 3). However, it has to be noted that the experimental lines assigned to H_2O_2 are weakened or disappear when going from pH 4.5 to pH 7.0 or higher. Thus, the corresponding lines may be absent in the vibrational spectra measured at pD 6.5 and 11.2 in the MIRIR study. Present results substantially agree, therefore, with the formation of H_2O_2 molecules and their assignment to vibrational lines as proposed in that study.

Some disagreement has been found instead between the present results and MIRIR results in the case of the OOH groups. A first difference concerns the assignment of the 838 cm^{-1} line to a neutral OOH surface group. Preliminarily, we observe that the isotopic shift of about 70 cm^{-1} proposed for the 838 cm^{-1} line (from 838 cm^{-1} to 740−770 cm^{-1}) in the MIRIR study seems quite unreasonable. Such a suggestion was justified by claiming the existence of similar shifts in deuterated H_2O_2.[36,41] On the contrary, the cited papers report only small, calculated shifts for deuterated H_2O_2, which agree with the present results showing that the H−D substitution has negligible effects on the O−O-stretching frequency in the H_2O_2 molecule; see Table 3. A further problem for the above assignment is that the band at 740−770 cm^{-1} is observed at pD 6.5 or higher, whereas the 838 cm^{-1} line (from which it derives) is not observed at pH 7.0 or higher. Thus, the isotopic shifts cannot be used to support the assignment of the 838 cm^{-1} line proposed in the MIRIR study. Theoretical and experimental results given in a study on Ti-silicalite[42] also invoked in favor of that assignment are not definitive. In addition, present results exclude the assignment of the 838 cm^{-1} line to a surface OOH group. On one hand, they indicate indeed that a neutral surface hydroperoxo group is unstable in the presence of water molecules. Moreover, even an isolated surface OOH group (i.e., without surrounding water molecules) is characterized by an O−O-stretching frequency of 1160 cm^{-1}, significantly higher than the 838 cm^{-1} one. On the other hand, the negative charge of the surface O_2^{-2} peroxo groups favors the capture of a H^+ ion and the formation of a surface OOH^- group which is stable in the presence of water molecules, but characterized by an O−O-stretching frequency of 971 cm^{-1} (see $OOH^- + nH_2O$ in Table 4), still too high with respect to the value of 838 cm^{-1}. Therefore, the present results do not agree with the assignment of the 838 cm^{-1} line to neutral or charged surface hydroperoxo groups. We can anticipate instead that further theoretical results (not reported here) suggest the assignment of that line to a different surface species related to water photooxidation.[33,38]

The value of 971 cm^{-1} estimated here for the O−O-stretching frequency of the $OOH^- + nH_2O$ is close to the experimental value of 943 cm^{-1}, thus suggesting that the OOH^- can contribute to the experimental line assigned to the O_2^{-2} peroxo group. It also has to be noted that H−D substitution has negligible effects on the 971 cm^{-1} frequency; see Table 4. Regarding the H-bending modes, the 1151 cm^{-1} frequency of $OOH^- + nH_2O$ can account for the experimental band at 1250−1120 cm^{-1}. For the calculated (but not observed) 1558 cm^{-1} frequency, it is possible to apply the considerations made above for the H_2O_2 molecules. Thus, present results support a coexistence of surface OOH^- groups, peroxo groups, and H_2O_2 molecules at low pH values. It should be also noted that the negative charge of the surface OOH^- groups proposed here favors their protonation and the formation of H_2O_2 molecules.

The above discussion does not permit the assignment of the 740−770 and 1023 cm^{-1} lines which will be discussed in the next section.

Hydroperoxo Radicals and OH Bridge Groups. Present results do not agree with the assignment of the 1023 cm^{-1} line proposed in the MIRIR study. This line is sensitive to the H substitution with D; that is, it should be related to a H vibrational mode. On the contrary, in the MIRIR study, the same line is assigned to the O−O-stretching frequency of hydroperoxo radicals present in the water solution. This would imply an appreciable isotopic shift of about 100 cm^{-1} (from 1023 cm^{-1} to the line at about 930 cm^{-1} in the spectra with D) for an O−O-stretching mode. However, such a shift is questionable because, as reported above, in the H_2O_2 molecule very small isotopic shifts of O−O vibrational modes are expected for H−D exchange.

The vibrational frequencies of [OOH•] and $[OOH^-]$ species have been calculated here in the cases of free molecules and molecules surrounded by water molecules, together with the corresponding isotopic shifts; see Table 4. In the case of free neutral and charged species, the values of the O−O-stretching frequencies are too large or too small, i.e., about 1119 and 755 cm^{-1}, respectively, when compared with the experimental value. Moreover, the corresponding isotopic shifts are smaller than 30 cm^{-1}. In the presence of surrounding water molecules, the O−O-stretching frequency of the neutral [OOH•] + nH_2O is equal to 1152 cm^{-1} and shifts of 5 cm^{-1} for H−D exchange. On the other hand, a negatively charged $[OOH^-]$ spontaneously reacts with a H_2O molecule by forming a H_2O_2 molecule and an $[OH^-]$ group. Thus, the above results do not agree with the proposed assignment of the 1023 cm^{-1} line to an O−O-stretching frequency. In the case of the neutral [OOH•] + nH_2O, a H-bending frequency of 1003 cm^{-1} is also estimated here that shifts at 739 cm^{-1} with D, thus being compatible with the experimental findings. However, such a frequency should be accompanied by an O−O-stretching frequency at 1147 cm^{-1} in the spectra with D at pD 6.5, not observed experimentally. All of the above results do not support, therefore, the assignment of the 1023 cm^{-1} line to either O−O or O−H vibrational modes of [OOH•] radicals in the solution phase. We propose instead that the above experimental line is related to the presence of surface OH bridge groups. The existence of such surface groups has been suggested in previous theoretical and experimental studies as a product of H_2O dissociation in the presence of oxygen vacancies.[6,10,11] Moreover, further theoretical results support the formation of surface OH-b groups as a product of the photooxidation of water molecules at the anatase surface.[38] Present results show that a surface OH-b behaves as a strong donor and is stable in its positively charged form at the surface of undoped anatase even in the presence of surrounding water molecules. In the case of the OH-b^++n H_2O, two H-bending frequencies at 1014 and 1075 cm^{-1} have been estimated that shift at 696 and 752 cm^{-1}, respectively, for H−D exchange. Both the 1014 and 1075 cm^{-1} (696 and 752 cm^{-1}) modes can

(41) Petterson, M.; Tuominen, S.; Räsänen, M. *J. Phys. Chem. A* **1997**, *101*, 1166.
(42) Lin, W.; Frei, H. *J. Am. Chem. Soc.* **2002**, *124*, 9292.

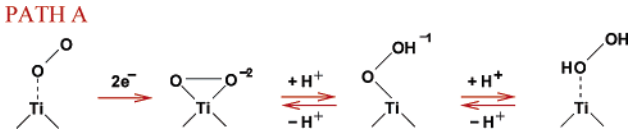

Figure 6. Reaction pathway for the O_2 photoreduction as proposed in the present study.

contribute to the 1023 cm^{-1} band (740 cm^{-1} band appearing in deuterated spectra). Alternatively, the 1075 cm^{-1} mode can contribute to the 1250−1120 cm^{-1} experimental band.

Intensities of the Vibrational Modes. A careful comparison of calculated intensities of the vibrational modes and simulated IR spectra with the results of the MIRIR study is reported in the Supporting Information. The calculated intensities alone give significant indications. The intensity of the O−O-stretching mode in the Ti(O_2^{-2}) peroxide is about twice that of the Ti−OOH^- species and much higher than that of H_2O_2. These results fully agree with our primary assignment of the 943 cm^{-1} experimental band to the Ti(O_2^{-2}) species as well as with a contribution of the Ti−OOH^- species to the same band. The 943 cm^{-1} experimental band is also the most intense one independently of the pH values, thus further supporting the above assignments. Appreciable intensities are calculated for the H-bending mode of Ti−OOH^- at 1151 cm^{-1} and for the OH-b^+ species mode at 1014 cm^{-1}, which contribute to the strong 1250−1120 and 1023 cm^{-1} experimental bands, respectively. A considerable intensity has been estimated also for the OH-b^+ species mode at 1075 cm^{-1} which can contribute to the 1023 cm^{-1} or, alternatively, to the 1250−1120 cm^{-1} experimental bands. All of these results support the assignments of the experimental IR bands to intermediates species as proposed in the present study, but for the H_2O_2 molecules. However, in this case, it is reasonable to assume that quite high concentrations of H_2O_2 molecules compensate for the low intensities calculated for the 898 cm^{-1} O−O-stretching and 1184 cm^{-1} H-bending modes corresponding to the 887 cm^{-1} and 1250−1120 cm^{-1} experimental bands, respectively. The reaction pathway proposed here, see Figure 6, indicates indeed that the formation of H_2O_2 molecules is strongly favored at low pH values, where the 887 cm^{-1} line is observed.

Conclusions

The assignments of the experimental vibrational lines to intermediates of the O_2 photoreduction as proposed here and in the MIRIR study are summarized in Table 6. Present estimates of the vibrational frequencies are in a very good agreement with the experimental lines once the formation of charged species and the effects of H bonds on the vibrational modes are taken into account. Even the calculated IR intensities fully support present assignments. A distinctive feature of the present theoretical picture is that *charged surface species* play a key role both in the line assignments and in the reaction scheme for the O_2 photoreduction proposed here; see Figure 6. In particular, the present results indicate a strong acceptor character of an O_2 molecule adsorbed on the anatase surface and a massive production of charged Ti(O_2^{-2}) peroxo groups upon UV irradiation. In turn, these Ti(O_2^{-2}) peroxo groups have significant effects on the formation of other intermediates. In fact, once formed, negatively charged peroxo groups easily capture a H^+ ion by forming surface Ti−OOH^- groups, thus giving rise to a chemical reaction favored by low pH values, in agreement with the experiment. In turn, the negative charge of the surface hydroperoxo group favors the capture of a second H^+ ion to form H_2O_2 molecules; see Figure 6, also in agreement with the experimental findings.

Table 6. Present Study vs MIRIR Study (ref 15) Assignments of the Experimental Vibrational Frequencies to Reaction Intermediates[a]

MIRIR study			present work		
lines	species	mode	lines	species	mode
943	Ti(O_2)	ν_{O-O}	958	Ti(O_2^{-2})	ν_{O-O}
	971	Ti−OOH^-			
887	H_2O_2	ν_{O-O}	898	H_2O_2	ν_{O-O}
838	Ti−OOH	ν_{O-O}	−	*b*	−
1250−1120	H_2O_2	δ_{O-H}	1184	H_2O_2	δ_{O-H}'
	Ti−OOH		1151	Ti−OOH^-	δ_{O-H}'
			(1075)	OH-b^+	δ_{O-H}
1023	OOH·	ν_{O-O}	1014	OH-b^+	δ_{O-H}'
			(1075)	OH-b^+	δ_{O-H}

[a] ν_{O-O} and δ_{O-H} indicate O−O-stretching and O−H-bending frequencies, respectively. δ'_{O-H} modes are peculiar bending modes induced by combined surface and water molecule effects. Alternative assignments are in parentheses. [b] Further theoretical results (not reported here) assign this line to an intermediate of the water photooxidation process.[38]

The most significant differences between the reaction schemes proposed here and in the MIRIR study can be easily appreciated by comparing Figure 1 with Figure 6. Path A in Figure 1 has been modified by specifying the charge of the involved species and by ruling out the formation of OH-t groups. Path B in Figure 1 has been totally removed.

Supporting Information Available: Preliminary results on short H bonds, calculated IR spectra and intensity analysis, charge of adsorbates, geometrical details of the adsorbed species, and details on the theoretical methods. This material is available free of charge via the Internet at http://pubs.acs.org.

Acknowledgment. We thank P. Giannozzi and M. Krack for helpful discussion and comments.

JA062145X